Easy and low-cost aqueous precipitation method to obtain $Cu_2ZnSn(S, Se)_4$ thin layers

Rafael Martí Valls[1,*], Teodora Stoyanova Lyubenova[1], Ivan Calvet Roures[1], Leonardo Oliveira[2], Diego Fraga Chiva[1], Juan B. Carda Castelló[1]

[1] Inorganic and Organic Chemistry Department, Universidad Jaume I, Av. Vicent de Sos Baynat s/n, 12071, Castellón de la Plana, Spain

[2] Department of aerospace science and technology, Institute of Aeronautics and Space - Materials Division, Praça Mal. Eduardo Gomes, 50, 12228-904, São José dos Campos, Brazil

* Corresponding Author: Tel: +34 964728234
E-mail address: vallsr@uji.es (Rafael Martí)

Abstract:

An easy method to obtain kesterite $Cu_2ZnSn(Se_{1-x},S_x)_4$ (CZTSSe) solid solution as an absorber for thin film photovoltaic solar cells is discussed in this report. Particular emphasis is directed toward the procedure´s steps of the CZTSSe preparation, as well as its structure and properties. For the preparation of CZTSSe an easy, low-cost and sustainable aqueous precipitation method that included chemical transformations of metal selenite precipitate, its reduction to metal selenides and further crystallization of kesterite, is applied. This procedure is more viable as avoids the use of selenization treatment and thus generation of toxic vapors and employs water as a solvent instead of organic compounds. In addition, the proposed procedure is very attractive way of preparation for industrial large-scale fabrication of the most promising absorber candidates for photovoltaic thin film solar cells.

Kesterite CZTSSe solid solution has been prepared and characterized in terms of chemical composition, structural and morphological transformations, as well as optical and electrical properties, confirming the viability and effectiveness of the applied process. The optimal electrical parameters obtained of the device are 21.5 mA/cm2, 532 mV, 42.8%., and 4.9% to short circuit current (Jsc), open circuit voltage (Voc), fill factor (FF), and efficiency (Eff.) respectively. Detailed description of each procedure steps and full characterization of the products, starting from as-prepared, intermediate and final compound is also exposed that could be very useful for any experimental scientist.

Keywords: CZTSSe, kesterite, precipitation, metal selenites, non-vacuum, thin film photovoltaics

Introduction

Thin film solar cells based on CIGS ($Cu(In_{1-x}Ga_x)Se_2$) absorber layer are noteworthy, reaching great efficiencies [1, 2] and can be consider as one of the most promising thin-film solar cells that have recently seen growing commercial success.

However, high production costs originated from the vacuum techniques employed to obtain the films and the rare element (gallium and indium) content makes this material undesirable for future industrial applications [3]. In contrast, the CZTSSe ($Cu_2ZnSn(S_{1-x},Se_x)_4$) is an attractive and well suited substitute to CIGS owing to sustainable (CZTS is composed of abundant and non-toxic elements) and low-cost production. Also, the CZTSSe exhibit an optimal and easily adjustable band gap that ranges between 1.1-1.5eV [4], a large absorption coefficient (>10^4 cm^{-1}) at few microns of thickness and the outgoings are lower than in CIGS (In and Ga are replaced by Zn and Sn) .

CZTSSe has been prepared by a variety of vacuum and non-vacuum techniques. Vacuum-based methods are dominant in the current CIGS industry, but in the past decade an increasing interest and progress in non-vacuum processes have been reaching owing to their potential lower costs and flexibility to coat large areas. Currently, the CZTSSe compound presents several problems during it preparation as following: volatility of certain compounds (e.g $Sn(S,Se)_2$) [5] that could be present during the kesterite formation, phase decomposition into binary compounds under reaction conditions [6, 7] or simultaneous formation of binary and ternary chalcogenide compounds (eg. Zn(S,Se), $CuSn(S,Se)_3$) [8, 9]. The non-vacuum processes have drawbacks for getting a single-phase material. This fact, increase the investigation on different preparation routs that could address these shortcomings.

A precursor-solution direct deposition (PSDD) ways of preparation are challenging non-vacuum methods that could solve some of the negative procedure problems. It is based on a direct obtaining of the CZTS layers after an annealing thermal treatment. The pure solution approach offers precursors homogeneity at a molecular scale and accordingly enables precise stoichiometric control and excellent film consistency, which

are necessary for low-cost and large-scale production. A world-record setting of CZTSSe solar cell with 12.6% energy conversion efficiency have been developed using a hydrazine-based ink [10, 11]. This ink is toxic and unstable, so require extreme conditions and equipment for storage that make this procedure unsuitable for applications. In this regards, many others hydrazine-free preparations route have been tested. Low- toxic organic solvents have been used for direct deposition of absorber layer as alcohols [12, 13], amines [14] and dimethyl sulfoxide (DMSO) [15] with high efficiency over 10% [16]. Even a water-ethanol mixture was developed with good results [17]. Xerogels followed by annealing process [18-21] was studied too. Recently, an improved sol-gel method achieved efficiencies of 8,2% [22]. This approach is very successful, but more complicate than the one that we describe. The gel process starts with metal acetates and thiourea (as sulfur raw material), thus the CZTS obtaining is design. After several procedure steps and selenization treatment, the mixed CZTSSe solid solution has been achieved. Good morphology has been attained expressed in improved film uniformity and this lead to higher electrical response. We are offering more simplified approach, starting with water co-precipitate product and after Doctor Blade disposition and sulfurization, the desired CZTSSe compound have been obtained. The advantages of our methodology is expressed in higher cost- effectiveness (cheaper reagents and solvents, less procedure steps) and industrially scalable (easy disposition procedure and no specific equipment is required) over the other fabrication procedures. In addition, selenization is totally avoided, thus it is environmental positive. Other routes based on nanoparticles [23], solvothermal [24-26], rotatory ball milling [27], microwave [28], hot-injection [25, 29-32] or non-injection methods [33], spray pyrolisis [34] have been also applied, but with inferior effectiveness for CZTSSe production.

All these solution-based methods highlights as a promising ways of preparation, due to it easy procedure that can be further re-scale at industrial level and it safety, and efficient material use of mainly low-toxic and sustainable components [35]. However, all above described methods (i.a using soft-chemistry solutions for the CZTSSe pepraration) starts from raw materials for the Cu_2ZnSnS_4 and then further selenized during annealing treatment (apart from hydrazine-containing process [10, 11]). Up to now, there are no references in the literature for using precursors (as metal selenites) for $Cu_2ZnSnS_{1-x}Se_4$, and thus avoiding the use of elemental selenium in the furnace during treatment (as it is

well-know that selenium vapors are toxic). Here, we are reporting the use of metal selenites as starting materials and their further sulfurization during thermal treatment, making this method of preparation more sustainable. An extra benefit of our way of preparation is the use of water as a solvent instead of difficulty to remove organic matter (e.g cleaning of oleylamine). The water is non-toxic, non-expensive, non-reactive in air solvent and can be applied with aqueous soluble, cheaper and large-scalable raw materials as metallic salts (nitrates, chlorides). By this way we avoid hazardous inorganic solvents (as hydrazine) or the use of expensive reagents (e.g metal acetates among others) and could solve drawbacks as volatility or inflammability. However, only few syntheses using water in combination with organic compounds have been reported up to now [36, 37].

In this work, we report a water –based easy, low cost and pollution-free method of CZTSSe preparation. It is based on co-precipitaion of metallic selenites precursors in aqueous medium [38-43]. After deposition by Doctor Blade technique, the layer is thermal treated in sulfur atmosphere. The CZTSSe solar cell with conversion efficiency of 4.9% was obtained and fully characterized in terms of composition, structure, microstructure and electrical properties.

Experimental

Synthesis of precursors

The reagents used for the synthesis were $Cu(NO_3)_2 \cdot 3H_2O$ (99%, Aldrich), $Zn(NO_3)_2 \cdot 6H_2O$ (99%, Fluka), $SnCl_4 \cdot 5H_2O$ (98%, Riedl-de-Haen), SeO_2 (99.8%, Aldrich) and ammonia solution NH_4OH (25%, Panreac) without previous purification. The metallic solution was prepared dissolving copper nitrate (2.52 mmol), zinc nitrate (1.71 mmol) and tin (1.42 mmol) chloride in 100 mL of distilled water. The metals ratio were selected as [Cu]/([Zn]+[Sn])= 0.8 and [Zn]/[Sn]=1.2 for avoiding additional phases formations [44, 45]). Separately, 10 mmol SeO_2 was dissolved in 50 mL of distilled water, and after both solutions were mixed. The ammonia solution was added up to pH 6-7 until the precipitate was achieved. The powder was washed with water and dried at room temperature.

Thin film preparation

Dispersion was prepared by mixing diethanolamine ($C_6H_{15}NO_3$ puriss. Riedel-de-Haën, abbreviated as DEA) and ethanol (C_2H_5OH Abs., Scharlau, abbreviated as EtOH) to the obtained precipitate. To improve crystallization process NaI solution (0,1% in distilled water) was added [46]**.** The obtained paste was deposited on Mo-coated soda-lime glass substrates by doctor Blade technique. The as-prepared CZTS film was pre-heated at 300ºC on a hot plate for 2 min and further heated in tubular furnace under sulfur and tin vapour atmosphere at 550°C with Ar as carrier gas. Finally, etching with KCN and NH_4S was performed to eliminate possible secondary phases [47].

The CZTSSe device were fabricated by adding the subsequent layers: CdS layer (60 nm) made by chemical bath deposition (CBD), followed by i-ZnO (50 nm) and ZnO:Al (450 nm) covering performed sequentially by DC-pulsed sputtering (model CT100, Alliance Concepts). For the optoelectronic characterization 3x3 mm^2 cells were scribed using a microdiamond scriber MR200 OEG.

Characterization techniques

Powder atomic composition was studied by Inductively Coupled Plasma-Mass Spectrometer (ICP-MS) Agilent 7500 C. Thin layer composition was obtained by X-ray Fluorescence (XRF) spectroscopy (Fisherscope XVD). The crystal structure of the materials was observed by X-ray powder diffraction (XRD) with a SIEMENS D5000D diffractometer equipped. The data were collected by step-scanning from 20 to 70º 2θ with a step size of 0.05º 2θ and 1s counting time per step. The X-ray photoelectron spectra (XPS) of the samples were measured with a SPECS apparatus equipped with a Phoibos 100 analyzer and a 5MCD detector. The morphology of powders and films were determined by Scanning Electron Microscopy (SEM), using a Leica-Zeiss JEOL 7001F, and Transmission Electron Microscopy (TEM) applying a JEOL 2100 microscope. Both equipments were equipped with a spectrometer for Energy dispersive X-ray energy spectroscopy (EDS). Phase analysis was carried out with Raman HR800-UV Horiba-Jobin Yvon spectrometer coupled with an Olympus metallographic microscope. Backscattering measurements were made using a 442 nm, 532 and 633 nm excitation wavelengths with the laser spot focused on the surface of samples. Optical absorption spectrum was recorded using VARIAN Cary 500 Scan UV-Vis-NIR spectrophotometer.

Current-voltage (I-V) characteristics of the solar cells were carried out using a solar simulator (Sun 3000 class AAA, Abet Technology) in standard illumination conditions: AM 1.5 and 100 mW/cm^2.

Results and discussion

CZTSSe powder was fabricated using a modified precipitation method described previously for CIGS absorber layer [40-43, 48]. The process is divided on three-stages: 1) precipitation of metal selenites; 2) paste preparation and deposition and 3) thermal treatment and kesterite crystallization. Each step of the synthesis procedure is described below.

Synthesis procedure

In order to determine the precipitation conditions, theoretical simulations were carrying out by HYDRA program (software for creating chemical equilibrium diagrams). Diagrams for ionic species as Cu^{2+}, Zn^{2+}, Sn^{4+}, $HSeO_3^-$ and SeO_3^{2-} are shown in Fig. 1.

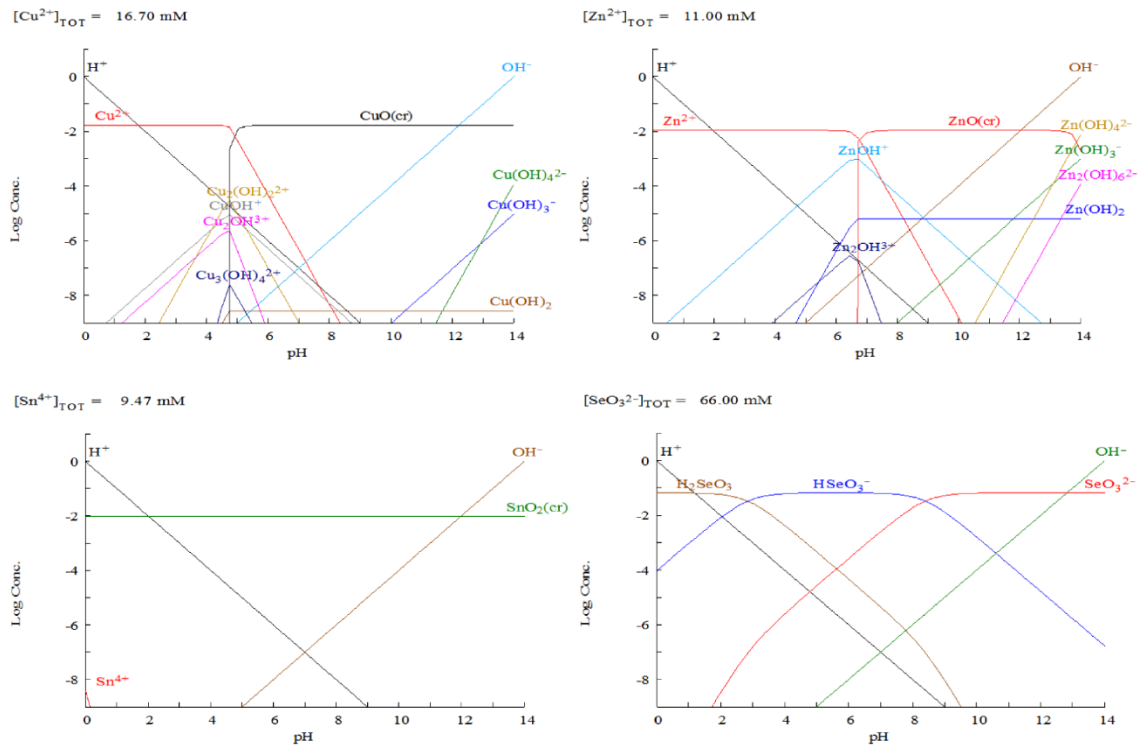

Figure 1. Phase equilibrium diagrams Cu^{2+}, Zn^{2+}, Sn^{4+}, SeO_3^{2-} (log Concentration vs pH)

The theoretical results display that Cu^{2+} and Zn^{2+} are dissolved until pH 6, while SeO_2 forms anionic species as $HSeO_3^-$ y SeO_3^{2-}. The Sn^{4+} precipitate mainly as SnO_2, $Sn(OH)_4$ or other oxide compounds [49, 50] along the whole range of pH from 0 to 14. In the literature is found that at pH 6-7, the predominant tin specie is as $Sn(OH)_4$ precipitate. Thus, hereafter and along the paper, the $Sn(OH)_4$ compound will be used to define the tin species obtained. However, we do not rule out the possibility the existence of other tin species or combination of them. Therefore, it is possible to get mixed metallic powder varying the pH value. Thus, at pH 6-7 the heterogeneous precipitates is obtained according to reaction (1):

$$Cu(NO_3)_2.3H_2O + Zn(NO_3)_2.6H_2O + SnCl_4.5H_2O + SeO_2 \xrightarrow{H_2O/NH_3} M_2(SeO_3)x.nH_2O + Sn(OH)_4 \quad (1)$$

where M= Cu, Zn

Morphology studies were performed applying SEM and TEM analysis (Fig. 2a and b). The SEM micrograph of the obtained precipitate (Fig. 2a) shows homogeneous amorphous agglomerates with average size of ~5 µm integrated by single particles of about 0.5µm. Closer view to the crystal morphology is performed by TEM (Fig. 2b). The image reveals grains with average dimensions of~25 nm. The amorphous structure of the powder is confirmed in the X-Ray diffraction spectrum (Fig. 3a).

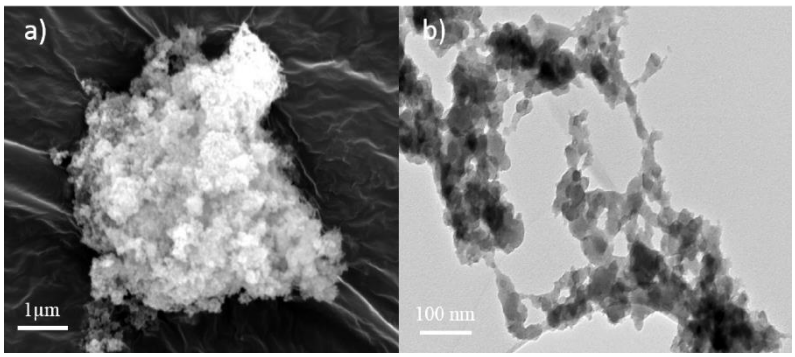

Figure 2. Micrographs of the precursor precipitate: (a) made by SEM and (b) performed by TEM

To check the chemical composition of the precipitate an EDS analysis was accomplished. The metal ratios of Cu/ (Zn+Sn) = 0.87 and Zn/Sn= 1.1 were similar to the initial stoichiometry of 0.8 and 1.2 respectively.

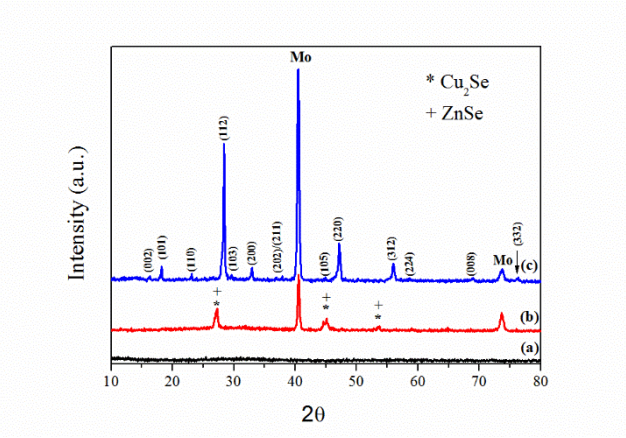

Figure 3: XRD spectra of: (a) as-prepared precursor precipitate; (b) pre-heated thin film; (c) thermal treated coating. Reflections indexed by hkl correspond to Cu_2ZnSnS_4 (JCPDS: 26-0575). Other peaks are related to: Cu_2Se (JCPDS:88-2044) and ZnSe (JCPDS: 37-1463).

To confirm the effectiveness of the procedure an ICP/MS analysis was made for the residual precipitation water. Tiny quantities (mol %) of Cu (0.58%) and Zn (0.022%) were detected that is related with completely specimen precipitation. The Sn quantity (0.0004%) was insignificant. Large Se amount in the residual water was detected (28.7%), due to $Sn(OH)_4$ precipitation instead of tin selenites ($Sn(SeO_3)_2$) species.

XPS of the Cu-Zn-Sn-Se as-synthesized powder was also performed (Fig. 4). The spectrum shows binding energy peaks related to $Zn2p_{3/2}$ at 1021.6 eV and $Sn3d_{3/2}$ at 486.4 eV [51], indicating that these cations maintain the initial oxidation state Zn^{2+} and Sn^{4+}. The peak observed at 58.64 eV is related to Se_{3d}, indicating that selenium oxidation state is 4+ (i.e. selenite species $SeO3^{2-}$) [51]. The reflections at 932 eV and 952 eV represent the levels $Cu2p_{3/2}$ and $Cu2p_{1/2}$, respectively. However, these reflections do not establish unambiguously the oxidation state of Cu. Cu^{1+} and Cu^{2+} have very similar response [51]. The XPS spectrum of Cu^{2+} is a broad peak centered at 942.5 eV with similar intensity to the $Cu2p_{1/2}$ [52]. However, this peak is not detected (Fig. 4 in-set) that suggests predominant existence of Cu^{1+} species. A small effect between $Cu2p_{3/2}$ and $Cu2p_{1/2}$ levels could be notice indicating a tiny quantity of Cu^{2+} [52] and resulting mixture of species. The reduction of Cu^{2+} to Cu^{1+} could be linked with the NH_3 addition as it is discussed in the literature [41, 53, 54].

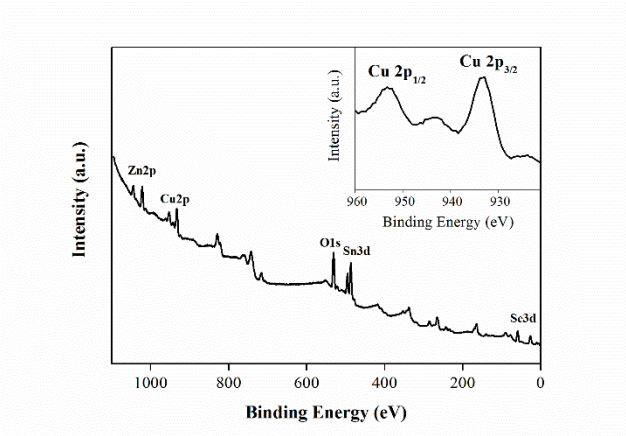

Figure 4: XPS spectrum of Cu-Zn-Sn-Se as-prepared powder. Inset view: zoomed section of Cu2p peaks

Paste preparation, thin film deposition

The prepared paste was deposited as a layer and pre-heated to incite the reduction from selenite to selenides according to the following reaction (2):

$$Cu_2(SeO_3).nH_2O + Zn(SeO_3).mH_2O + Sn(OH)_4 + C_6H_{15}NO_3 \xrightarrow{\Delta} Cu_2Se + ZnSe + SnO_2 + by-products \quad (2)$$

For this purpose, amines-type compounds (as DEA) was used [55, 56]. The effectiveness of the pre-heating on a hot plate step is explored by the XDR spectrum (Fig. 3b). The main reflections at 27.2º, 45 º and 53.6 º could be associated to ZnSe (JCPDS 37-1463) or Cu_2Se (JCPDS 88-2044) compounds due to their similar crystallographic features. It is uncertain to determine the exact presented crystal phases. Thus, the Raman spectroscopy was performed to clarify the existence of binary compounds in the sample at excitation longwave of 442 nm, 532 nm and 633 nm (Fig. 5, as-prepared and thermal treated samples). For the Raman spectra at 532nm and 633nm (Table 1) peaks at around 195cm^{-1} and 260-261 cm^{-1} was detected that be linked to Cu_2Se [57]. The rest of the reflections and reference literature are summarized in the Table 1.

Table 1. Summary of the Raman reflections present in the synthesized CZTSSe sample (as-prepared and after thermal treatment) at 442nm, 532nm and 633 nm excitation wavelengths (ordered from high to low intensity).

Laser (cm^{-1})	Sample	Raman scattering peak (cm^{-1})	References
442	as-prepared	260 (Cu_2Se)	[57]
	thermal treated	338, 287, 366, 238, 142 (CZTS)	[58-60]
532	as-prepared	260, 196 (Cu_2Se)	[57]

	thermal treated	338, 288, 366, 238, 166 (CZTS)	[58-60]
633	as-prepared	261, 196 (Cu_2Se)	[57]
	thermal treated	337, 366, 287, 238, 166, 142 (CZTS) 264 (Cu_2S), 303 (Sn_2S_3)	[58-61]

Elemental analysis made by X-Ray Fluorescence (XRF) confirms the initial stoichiometric composition (Cu/ (Zn+Sn) = 0.86 and Zn/Sn= 1.1) (Table 2) and the synthesis attainment.

Table 2. Chemical composition of the developed sample: FRX of as-prepared layer; FRX and EDS of final treated CZTSSe absorber layer.

	Cu/(Zn + Sn)	**Zn/Sn**	**Se/(S + Se)**
FRX (as-prepared)	0.86	1.1	-
FRX (final)	0.93	1.09	0.84
EDS	1.02	1.64	0.85

CZTSSe crystallization

The XRD pattern of crystallized absorber film (Fig. 3 (b)) exhibit several diffraction peaks. The most intense ones correspond to (112), (220) and (312) and could be related to Cu_2ZnSnS_4 (JCPDS: 26-0575). Leftward peak shifting of the sample reflections comparing to the standard pattern (JCPDS: 26-0575) deduces a partial selenium replacement by sulphur and consequently a solid solution formation of $Cu_2ZnSn(S_xSe_{1-x})_4$. Suggestion for the reaction mechanism can be made according the following reaction:

$$Cu_2Se + ZnSe + SnO_2 \xrightarrow{Sulphur} Cu_2ZnSn(S,Se)_4 \quad (3)$$

Many secondary phases are general possible in quaternary compounds like CZTS and CZTSe. Their presence can affect the solar cell performance. Secondary phases can provide shunting current paths through the solar cell or act as recombination centers, both degrading solar cell performance. Thus, detailed characterization by Raman spectroscopy is made to identify the presence of secondary phases (e.g Cu_2S, ZnS or Cu_2SnS_3) that are difficult to be discern through XRD, due to overlaping with the reflection of Cu_2ZnSnS_4 [8, 62].

The Raman measurements in the three longwave (Table 1) confirm the kesterite Cu_2ZnSnS_4 existence with the peaks centered at 337-338 cm^{-1} (main), 287-288 cm^{-1} and

366 cm^{-1} [58]. Others reflections present could be also ascribed to Cu_2ZnSnS_4 as 238 cm^{-1} (442 nm, 532nm and 633 nm) [59] , 166 cm^{-1} (532nm and 633 nm) and 142 cm^{-1} (442 nm and 633 nm) [60]. Measurements at 633nm present extra peaks at 264 cm^{-1} and 303 cm^{-1} which could be related to Cu_2S [58] and Sn_2S_3 [61] respectively. Etching treatments with KCN and NH_4S was performed for elimination of the undesirable secondary phases [47].

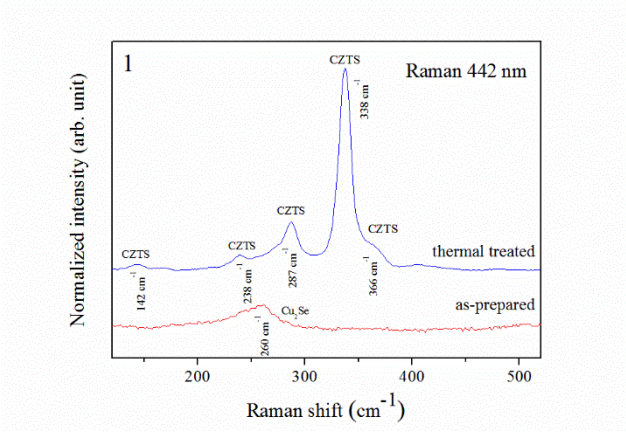

Figure 5(1): Raman spectrum of CZTS layers before and after thermal treatment at 442 nm excitation wavelength.

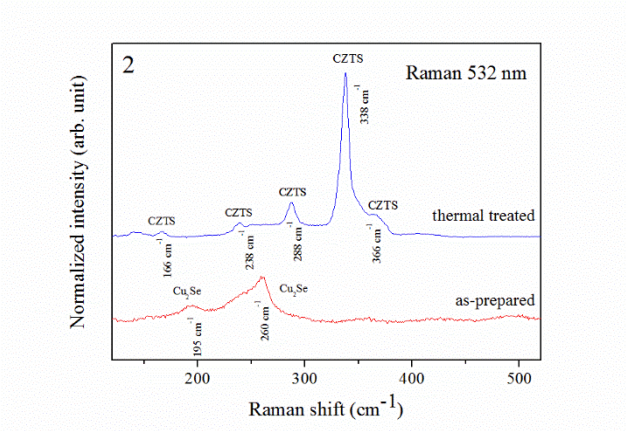

Figure 5(2): Raman spectrum of CZTS layers before and after thermal treatment at 532 nm excitation wavelength.

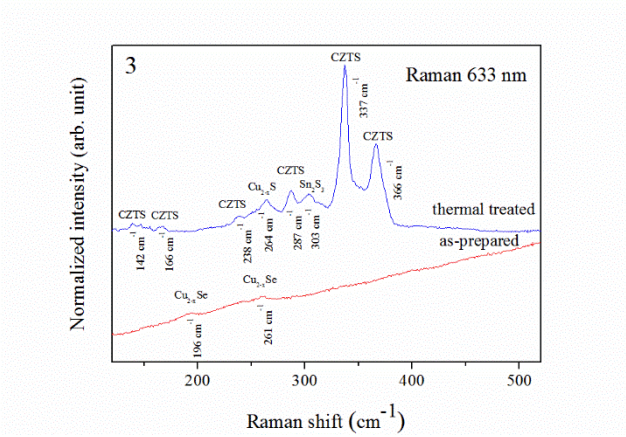

Figure 5(3): Raman spectrum of CZTS layers before and after thermal treatment at 633 nm excitation wavelength.

SEM surface micrograph of absorber (Fig. 6a) shows compact layer with a few cracks and crystals ranging between 300 nm-1,2 µm. The stack micrograph (Fig. 6b) displays CZTSSe absorber layer with dimensions of 1.5 µm that differ in microstructure. The bottom morphology contains carbon-embedded kesterite particles with 0.5 µm thicknesses (labeled as CZTS1), are usually observed when organic substances are applied [63, 64]. The upper area is made of kesterite crystals with ~1 µm size (labeled as CZTS2). The thin film elemental composition is checked in Table 2. Slightly differences from the initial composition are observed due to possible Sn volatilization during treatment [65].

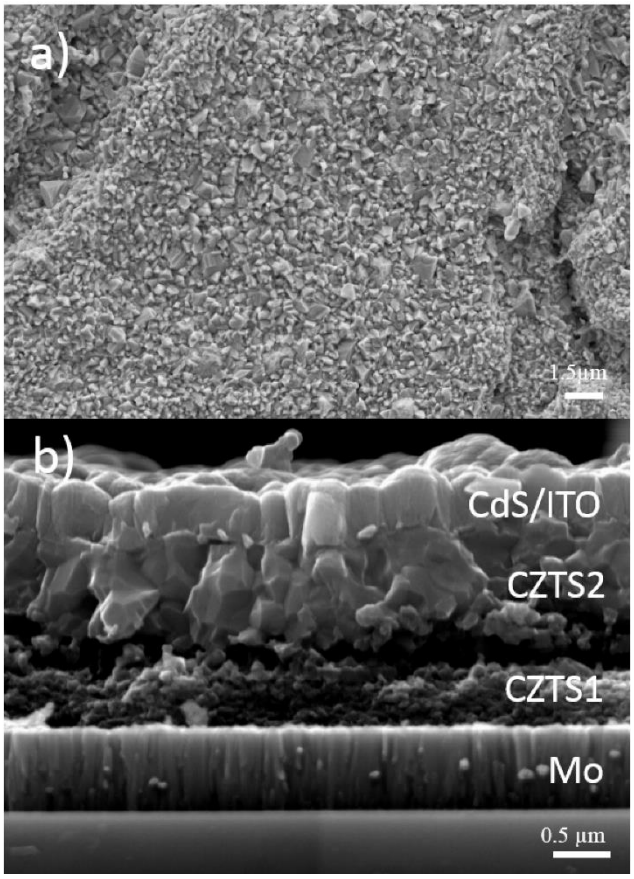

Figure 6: SEM superficial section of a treated at 550ºC film (upper) and SEM view of a final solar cell assembly (lower).

Band GAP value of 1.33eV is measured by UV-VIS-NIR spectroscopy (Fig. 7). The obtained energy GAP could be associated with a solid solution formation of CZTSSe, introducing sulfur in the kesterite structure as the band gap of $Cu2ZnSnSe_4$ is varying between 0.95-1.0 eV and the band gap of $Cu2ZnSnS_4$ is between 1.45-1.5 eV [4, 66].

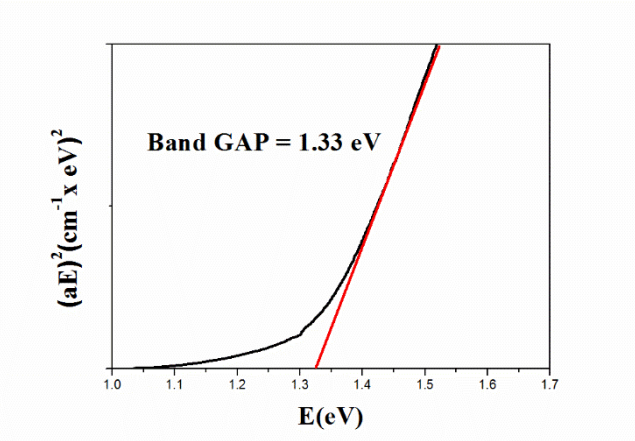

Figure 7: Band GAP energy calculations of CZTSSe layer

The current-voltage (I-V) characteristics for the CZTSSe solar cell measured under one sun illumination are shown in Fig. 8. The as-fabricated device shows an efficiency of 4.89 % and cell parameters V_{OC} = 532 mV, J_{SC} = 21.5 mA/cm^2 and FF = 42.8%. The high V_{OC} (~500 mV) was measured in different areas and this results also confirm the sulphur substitution in the crystal lattice [11, 31, 67-72]. However, the lower efficiency and fill factor are related with parasitic resistance (R_S and R_{SH}) values, perhaps due to the presence of some cracks in the thin film surface. To solve these harms, morphology improvement is required (e.g avoiding the pre-heating step, slower velocity or changes in the annealing step and deposition). Further methodology enhancements are taking into account for future studies.

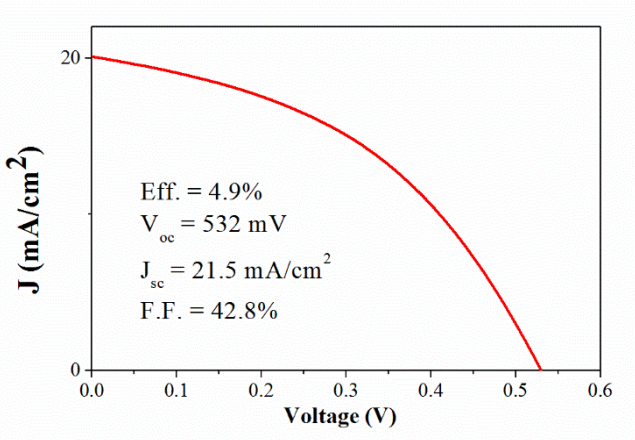

Figure 8: I-V curve of the best CZTSSe solar cell under illumination

Conclusion

Kesterite $Cu_2ZnSn(Se_{1-x},S_x)_4$ solid solution have been successfully achieved. The $Cu_2ZnSnSe_4$ have been firstly designed and then sulfurization is applied during heating. This panning provides a pollution-free way of preparation, avoiding selenium vapours during treatment. The chemical composition of the amorphous selenites nano-powder fits with the initial stoichiometry and confirms the effectiveness of the precipitation process. Adequate layer deposition is performed expressed in well crystalized coating morphology. However, some isolated surface cracks are observed that harms the final efficiency. The CZTSSe solid solution is confirmed also by the band gap (1.33eV) and electrical measurements (V_{OC} =532mV). Device efficiency of 4.9% was attained. Detailed description of each procedure steps and full characterization of the products, starting from as-prepared, intermediate and final compound is also exposed that could be very useful for any experimental scientist. The proposed procedure is very attractive way of preparation for industrial fabrication of the most promising absorber candidates for photovoltaic thin film solar cells.

Acknowledgments

The authors would like to acknowledge the financial support of the Spanish Ministry of Economy and Competitiveness under the programs RETOS-COLABORACION (RTC-2014-2294-3) and RETOS-INVESTIGACIÓN (ENE2013-49136-C4-2-R). We also appreciate the characterization assistance of Central Service of Scientific Instrumentation (SCIC) at the University Jaume I and Catalonia Institute for Energy Research (IREC) for them help in the Raman measurements. Finally, R. Martí would like to thank the support of university Jaume I through FPI-UJI grant.

Notes and References

1. J. Gifford, *Journal*, 2015.
2. T. M. Friedlmeier, P. Jackson, A. Bauer, D. Hariskos, O. Kiowski, R. Wuerz and M. Powalla, *IEEE Journal of Photovoltaics*, 2015, **5**, 1487-1491.
3. J. D. Beach and B. E. McCandless, *MRS Bulletin*, 2007, **32**, 225-229.
4. R. Haight, A. Barkhouse, O. Gunawan, B. Shin, M. Copel, M. Hopstaken and D. B. Mitzi, *Applied Physics Letters*, 2011, **98**, 253502.
5. A. Weber, R. Mainz and H. W. Schock, *Journal of Applied Physics*, 2010, **107**, 013516.

6. S. Lopez-Marino, M. Placidi, A. Perez-Tomas, J. Llobet, V. Izquierdo-Roca, X. Fontane, A. Fairbrother, M. Espindola-Rodriguez, D. Sylla, A. Perez-Rodriguez and E. Saucedo, *Journal of Materials Chemistry A*, 2013, **1**, 8338-8343.
7. J. J. Scragg, P. J. Dale, D. Colombara and L. M. Peter, *ChemPhysChem*, 2012, **13**, 3035-3046.
8. X. Fontané, L. Calvo-Barrio, V. Izquierdo-Roca, E. Saucedo, A. Pérez-Rodriguez, J. R. Morante, D. M. Berg, P. J. Dale and S. Siebentritt, *Applied Physics Letters*, 2011, **98**, 181905.
9. J. Just, D. Lützenkirchen-Hecht, R. Frahm, S. Schorr and T. Unold, *Applied Physics Letters*, 2011, **99**, 262105.
10. T. K. Todorov, K. B. Reuter and D. B. Mitzi, *Advanced Materials*, 2010, **22**, E156-E159.
11. W. Wang, M. T. Winkler, O. Gunawan, T. Gokmen, T. K. Todorov, Y. Zhu and D. B. Mitzi, *Advanced Energy Materials*, 2014, **4**, n/a-n/a.
12. T. K. Chaudhuri and D. Tiwari, *Solar Energy Materials and Solar Cells*, 2012, **101**, 46-50.
13. R. Zhang, S. M. Szczepaniak, N. J. Carter, C. A. Handwerker and R. Agrawal, *Chemistry of Materials*, 2015, **27**, 2114-2120.
14. Y. Sun, Y. Zhang, H. Wang, M. Xie, K. Zong, H. Zheng, Y. Shu, J. Liu, H. Yan, M. Zhu and W. Lau, *Journal of Materials Chemistry A*, 2013, **1**, 6880-6887.
15. W. Ki and H. W. Hillhouse, *Advanced Energy Materials*, 2011, **1**, 732-735.
16. T. Schnabel, Abzieher, T., Friedlmeier, T.M., Ahlswede, E., *Photovoltaics, IEEE Journal of* 2015, **5**, 670-675.
17. M. Jiang, F. Lan, X. Yan and G. Li, *physica status solidi (RRL) – Rapid Research Letters*, 2014, **8**, 223-227.
18. K. Tanaka, Y. Fukui, N. Moritake and H. Uchiki, *Solar Energy Materials and Solar Cells*, 2011, **95**, 838-842.
19. K. Tanaka, M. Oonuki, N. Moritake and H. Uchiki, *Solar Energy Materials and Solar Cells*, 2009, **93**, 583-587.
20. C. M. Fella, A. R. Uhl, Y. E. Romanyuk and A. N. Tiwari, *physica status solidi (a)*, 2012, **209**, 1043-1048.
21. N. Moritake, Y. Fukui, M. Oonuki, K. Tanaka and H. Uchiki, *physica status solidi (c)*, 2009, **6**, 1233-1236.
22. F. Liu, F. Zeng, N. Song, L. Jiang, Z. Han, Z. Su, C. Yan, X. Wen, X. Hao and Y. Liu, *ACS Applied Materials & Interfaces*, 2015, **7**, 14376-14383.
23. C. K. Miskin, W.-C. Yang, C. J. Hages, N. J. Carter, C. S. Joglekar, E. A. Stach and R. Agrawal, *Progress in Photovoltaics: Research and Applications*, 2015, **23**, 654-659.
24. M. Cao and Y. Shen, *Journal of Crystal Growth*, 2011, **318**, 1117-1120.
25. D. Fraga, *Síntesis de kesterita Cu2ZnSn(S,Se)4 mediante métodos de hot-injection y solvotermal*, Sociedad Española de Cerámica y Vidrio, 2014.
26. R. M. D. Fraga, T. Lyubenova, L. Oliveira, A. Rey, S. Kozhukharov, J. Carda, *Annual Proceedings of Angel Kanchev University of Ruse (Bulgaria)*, 2012, **51**, 46–49.
27. Z. Zhou, Y. Wang, D. Xu and Y. Zhang, *Solar Energy Materials and Solar Cells*, 2010, **94**, 2042-2045.
28. S. W. Shin, J. H. Han, C. Y. Park, A. V. Moholkar, J. Y. Lee and J. H. Kim, *Journal of Alloys and Compounds*, 2012, **516**, 96-101.
29. H. Wei, W. Guo, Y. Sun, Z. Yang and Y. Zhang, *Materials Letters*, 2010, **64**, 1424-1426.

30. S. C. Riha, B. A. Parkinson and A. L. Prieto, *Journal of the American Chemical Society*, 2009, **131**, 12054-12055.
31. Q. Guo, G. M. Ford, W.-C. Yang, B. C. Walker, E. A. Stach, H. W. Hillhouse and R. Agrawal, *Journal of the American Chemical Society*, 2010, **132**, 17384-17386.
32. T. Rath, W. Haas, A. Pein, R. Saf, E. Maier, B. Kunert, F. Hofer, R. Resel and G. Trimmel, *Solar Energy Materials and Solar Cells*, 2012, **101**, 87-94.
33. W. Liu, M. Wu, L. Yan, R. Zhou, S. Si, S. Zhang and Q. Zhang, *Materials Letters*, 2011, **65**, 2554-2557.
34. T. H. Nguyen, W. Septina, S. Fujikawa, F. Jiang, T. Harada and S. Ikeda, *RSC Advances*, 2015, **5**, 77565-77571.
35. D. B. Mitzi, O. Gunawan, T. K. Todorov, K. Wang and S. Guha, *Solar Energy Materials and Solar Cells*, 2011, **95**, 1421-1436.
36. D. Tang, Q. Wang, F. Liu, L. Zhao, Z. Han, K. Sun, Y. Lai, J. Li and Y. Liu, *Surface and Coatings Technology*, 2013, **232**, 53-59.
37. S. k. Verma, V. Agrawal, K. Jain, R. Pasricha and S. Chand, *Journal of Nanoparticles*, 2013, **2013**, 7.
38. S. D. Nguyen and P. S. Halasyamani, *Inorganic Chemistry*, 2013, **52**, 2637-2647.
39. P. Amorós, M. D. Marcos, M. Roca, A. Beltrán-Porter and D. Beltrán-Porter, *Journal of Solid State Chemistry*, 1996, **126**, 169-176.
40. C. J. B. Cardá, L. P. Escribano, T. T. Krassimirov, D. Lincot and E. Chassaing, *Journal*, 2015.
41. R. Martí, L. Oliveira, T. S. Lyubenova, T. Todorov, E. Chassaing, D. Lincot and J. B. Carda, *Journal of Alloys and Compounds*, 2015, **650**, 907-911.
42. D. Fraga, T. S. Lyubenova, A. Rey, I. Calvet, R. Martí and J. B. Carda, *International Journal of Applied Ceramic Technology*, 2015, **12**, 728-737.
43. I. Calvet, E. Barrachina, R. Martí, D. Fraga, T. Stoyanova Lyubenova and J. B. Carda, *Materials Letters*, 2015, **161**, 636-639.
44. H. Katagiri, K. Jimbo, W. S. Maw, K. Oishi, M. Yamazaki, H. Araki and A. Takeuchi, *Thin Solid Films*, 2009, **517**, 2455-2460.
45. A. Ennaoui, M. Lux-Steiner, A. Weber, D. Abou-Ras, I. Kötschau, H. W. Schock, R. Schurr, A. Hölzing, S. Jost, R. Hock, T. Voß, J. Schulze and A. Kirbs, *Thin Solid Films*, 2009, **517**, 2511-2514.
46. T. Prabhakar and N. Jampana, *Solar Energy Materials and Solar Cells*, 2011, **95**, 1001-1004.
47. H. Xie, Y. Sánchez, S. López-Marino, M. Espíndola-Rodríguez, M. Neuschitzer, D. Sylla, A. Fairbrother, V. Izquierdo-Roca, A. Pérez-Rodríguez and E. Saucedo, *ACS Applied Materials & Interfaces*, 2014, **6**, 12744-12751.
48. T. K. Todorov, Universitat Jaume I, 2008.
49. B. Zhou, S. Hann, R. Raja, G. A. Somorjai, S. American Chemical and Meeting, Nanotechnology in catalysis, http://public.eblib.com/choice/publicfullrecord.aspx?p=372358).
50. S. Sakka, *Handbook of sol-gel science and technology. 1. Sol-gel processing*, Kluwer Academic Publishers, 2005.
51. W. H. R. C. D. Wagner, L. E. Davis, J. F. Moulder, G. E. Muilinberg, *Handbook of X-Ray Photoelectron Spectroscopy*, Minnesota, 1973.
52. J. P. Espinós, J. Morales, A. Barranco, A. Caballero, J. P. Holgado and A. R. González-Elipe, *The Journal of Physical Chemistry B*, 2002, **106**, 6921-6929.

53. F. Nishida, T. Yamada, N. Suzuki, T. Takeda, T. Yanagihara, K. Adachi, T. Asanabe, K. Ohsato and K. Tsuda, *Journal*, 1978.
54. T. Curtin, F. O' Regan, C. Deconinck, N. Knüttle and B. K. Hodnett, *Catalysis Today*, 2000, **55**, 189-195.
55. W. C. Benzing, J. B. Conn, J. V. Magee and E. J. Sheehan, *Journal of the American Chemical Society*, 1958, **80**, 2657-2659.
56. J. J. Lin and Y. H. Wu, *Journal*, 2012.
57. O. Ramdani, J. F. Guillemoles, D. Lincot, P. P. Grand, E. Chassaing, O. Kerrec and E. Rzepka, *Thin Solid Films*, 2007, **515**, 5909-5912.
58. P. A. Fernandes, P. M. P. Salomé and A. F. da Cunha, *Journal of Alloys and Compounds*, 2011, **509**, 7600-7606.
59. E. Mkawi, K. Ibrahim, M. Ali and A. S. Mohamed, *Int. J. Electrochem. Sci*, 2013, **8**, 359-368.
60. X. Fontane, Universidad de Barcelona, 2013
61. P. A. Fernandes, P. M. P. Salomé and A. F. da Cunha, *Thin Solid Films*, 2009, **517**, 2519-2523.
62. B. G. Mendis, M. C. J. Goodman, J. D. Major, A. A. Taylor, K. Durose and D. P. Halliday, *Journal of Applied Physics*, 2012, **112**, 124508.
63. Y. E. Romanyuk, C. M. Fella, A. R. Uhl, M. Werner, A. N. Tiwari, T. Schnabel and E. Ahlswede, *Solar Energy Materials and Solar Cells*, 2013, **119**, 181-189.
64. T. Schnabel, M. Löw and E. Ahlswede, *Solar Energy Materials and Solar Cells*, 2013, **117**, 324-328.
65. W. Yang, H.-S. Duan, B. Bob, H. Zhou, B. Lei, C.-H. Chung, S.-H. Li, W. W. Hou and Y. Yang, *Advanced Materials*, 2012, **24**, 6323-6329.
66. S. Chen, A. Walsh, J.-H. Yang, X. G. Gong, L. Sun, P.-X. Yang, J.-H. Chu and S.-H. Wei, *Physical Review B*, 2011, **83**, 125201.
67. H. Xin, J. K. Katahara, I. L. Braly and H. W. Hillhouse, *Advanced Energy Materials*, 2014, **4**, n/a-n/a.
68. M. Werner, C. M. Sutter-Fella, Y. E. Romanyuk and A. N. Tiwari, *Thin Solid Films*, 2015, **582**, 308-312.
69. C. K. Miskin, W.-C. Yang, C. J. Hages, N. J. Carter, C. S. Joglekar, E. A. Stach and R. Agrawal, *Progress in Photovoltaics: Research and Applications*, 2014, DOI: 10.1002/pip.2472, n/a-n/a.
70. G. Brammertz, M. Buffière, S. Oueslati, H. ElAnzeery, K. Ben Messaoud, S. Sahayaraj, C. Köble, M. Meuris and J. Poortmans, *Applied Physics Letters*, 2013, **103**, 163904.
71. B. Shin, Y. Zhu, N. A. Bojarczuk, S. Jay Chey and S. Guha, *Applied Physics Letters*, 2012, **101**, 053903.
72. B. Shin, O. Gunawan, Y. Zhu, N. A. Bojarczuk, S. J. Chey and S. Guha, *Progress in Photovoltaics: Research and Applications*, 2013, **21**, 72-76.